

Learning from success, not catastrophe: using counterfactual analysis to highlight successful disaster risk reduction interventions

Maricar L. Rabonza^{1,2*}, Yolanda C. Lin³ and David Lallemand^{1,2}

¹Asian School of the Environment, Nanyang Technological University, Singapore

²Earth Observatory of Singapore, Nanyang Technological University, Singapore

³Department of Geography and Environmental Studies, University of New Mexico, Albuquerque, NM, USA

Correspondence*:

Maricar L. Rabonza

50 Nanyang Ave, Block N2-01c-63, 639798, Singapore

MARICARL001@e.ntu.edu.sg

2 ABSTRACT

In the aftermath of a disaster, news and research attention is focused almost entirely on catastrophic narratives and the various drivers that may have led to the disaster. Learning from failure is essential to preventing future disasters. However, hyperfixation on the catastrophe obscures potential successes at the local scale, which could serve as important examples and learning resources in effective risk mitigation. To highlight effective risk mitigation actions that would otherwise remain unnoticed, we propose the use of probabilistic downward counterfactual analysis. This approach uses counterfactual modelling of a past hazard event with consequences made worse (i.e. downward counterfactual) by the absence of the mitigation intervention. The approach follows probabilistic risk analysis procedures where uncertainties in the simulated events and outcomes are accounted for and propagated. We demonstrate the method using a case study of Nepal's School Earthquake Safety Program, implemented before the 2015 M_w 7.8 Gorkha earthquake. Using a school building database for Kathmandu Valley, Nepal, we present two applications: (1) the quantification of lives saved during the Gorkha earthquake as a result of the retrofitting of schools in Kathmandu Valley since 1999, (2) the quantification of the annual expected lives saved if the pilot retrofitting program was extended to all school buildings in Kathmandu Valley based on a probabilistic seismic hazard model. The shift in focus from realised outcome to counterfactual alternative enables the quantification of the benefits of risk reduction programs amidst disaster, or for a hazard that has yet to unfold. Such quantified counterfactual analysis can be used to celebrate successful risk reduction interventions, providing important positive reinforcement to decision-makers with political bravery to commit to the implementation of effective measures.

Keywords: counterfactual analysis, probabilistic risk, disaster risk reduction, risk framework, school earthquake safety

1 INTRODUCTION

Success in disaster risk management (DRM) means that natural hazard events do not turn into disasters, and communities continue to function and be resilient to shocks and stresses from hazards. Since the extent of

27 a disaster can be characterised by loss of life and disruptions to the physical, built and social environments,
28 (Mileti, 1999; Smith, 2005; Moore, 1958), the extent of success of risk reduction interventions manifest
29 primarily as reduced impact. As such, success is measured as an *absence* (e.g. no damage, fewer casualties,
30 etc). This poses a challenge for recognising and incentivising important investments in DRM interventions
31 since they are made invisible by their very nature.

32 In the aftermath of earthquakes, storms, and floods, narratives of catastrophe dominate the interest of
33 media, political and research communities. However, this hyper-fixation on the catastrophe can obscure
34 important successes amid the broader disaster. Another challenge is to recognize successful interventions if
35 the hazard they were designed for has not yet occurred. This happens when we rely on a disaster occurrence
36 to make mitigation benefits visible. For extreme and rare hazard events, for example, the benefits of
37 risk reduction may manifest only in the distant future. Because of the significant time delay between the
38 interventions and their benefits being manifested, such interventions can be perceived as unsuccessful or
39 squandered until the event occurs. These are two of the challenges described in Lallemand and Rabonza et al.
40 (2022) where successful DRM interventions are made invisible: “invisible success in the midst of broader
41 disaster”, and “invisible success due to yet unrealised benefits.” These *invisible successes* of mitigation
42 interventions are related to a cognitive tendency called *outcome bias* - the tendency to judge the quality of
43 a decision by the outcome alone (Robson, 2019).

44 To address outcome bias, we propose a *probabilistic downward counterfactual analysis* approach. It
45 relies on comparing the outcome of a realised event in which a risk reduction was implemented, to an
46 alternative branch of history (i.e. *counterfactual*) in which the disaster risk reduction intervention was not
47 implemented. Throughout the paper, we use the term *realised* to refer to events or outcomes that transpired
48 (in juxtaposition to *counterfactual*), in alignment with prior literature on probability and counterfactual
49 analysis (Roese, 1997). An imagined scenario where an intervention is absent is considered a *downward*
50 *counterfactual* because the assumed outcome is worse than what was observed in reality (Roese, 1997).
51 This is in contrast with an *upward counterfactual* where the assumed outcome is better. Probabilistic
52 downward counterfactual analysis is *probabilistic* in that it follows probabilistic risk analysis procedures to
53 propagate and account for uncertainties in events and outcomes. In this paper, we present two applications
54 of probabilistic downward counterfactual analysis to highlight the effectiveness of risk reduction in terms of
55 probabilistic lives saved. The first application estimates the benefits of an intervention in a past earthquake
56 through comparison of fatalities modelled without the risk intervention and actual fatalities. The second
57 application estimates the probabilistic benefits of a mitigation for a hazard that has not yet occurred. Instead
58 of an actual past event, a hazard model is used to calculate the intervention’s benefits.

59 The paper’s main contribution is in combining the probabilistic risk analysis framework and counterfactual
60 analysis to calculate and highlight lives saved from successful disaster risk reduction interventions, that
61 otherwise go unnoticed. The significance and novelty of this work is in shifting our perception of the
62 benefits of risk reduction intervention, by using an appropriate counterfactual scenario as the baseline
63 against which to calculate and judge these benefits. Rather than focusing entirely on realised outcomes, the
64 analysis of counterfactual outcomes shines light on the value of a mitigation intervention by demonstrating
65 what would have been without such intervention. Downward counterfactual risk analysis has only so
66 far been used to identify potential worse impacts for the purpose of insurance, preparedness, or future
67 mitigation (e.g. Lin et al., 2020; Aspinall and Woo, 2019; Woo, 2019; Woo and Mignan, 2018; Shepherd
68 et al., 2018; Woo et al., 2017; Oughton et al., 2019; Aspinall and Woo, 2019). This study pioneers a
69 systematic approach to creating incentives for good decision-making on the basis of probabilistic risk. The
70 quantification of probabilistic lives saved by effective risk reduction programs in a major hazard event

71 serves as a powerful indicator of the intervention's success that would otherwise remain unnoticed amidst a
 72 disaster. In addition, the calculated probabilistic benefits of an intervention provide important incentive
 73 and encouragement to decision-makers committed to implementing effective measures even if the benefits
 74 are not materialized yet by the occurrence of a hazard event. Altogether, this work is a new domain of
 75 application of counterfactual analysis with much potential across the broad spectrum of hazards.

76 The proposed framework has significant implications to multiple potential stakeholders. For policymakers,
 77 there is currently little political capital gained from investing in resilience if the benefits of such investments
 78 are invisible. By having the benefits of these investments visible to their constituents, policymakers will
 79 be incentivised for risk-informed decision-making. For donors and funders, this framework would enable
 80 them to monitor progress in terms of probabilistic impacts reduced, even if such benefits remain unrealized
 81 until a disaster strikes. For disaster risk management practitioners, while it is important to learn from
 82 failures, it is equally important to learn from successes, and share them broadly so they can be emulated,
 83 scaled, and adapted in other contexts where they are needed. Importantly, it also provides a mechanism to
 84 recognise and elevate the important, humble, long-term, and dedicated work conducted by many to keep
 85 our communities safe, even when their work is unseen.

86 The paper is organized as follows. Section 2 introduces the proposed framework in the context of
 87 probabilistic risk analysis. In Section 3, we describe the earthquake risk intervention that will be the focus
 88 of our two applications: the school earthquake retrofitting program in Nepal, implemented before the
 89 2015 M_w 7.8 Gorkha earthquake. In the subsequent sections, we present the methods (Section 4) and two
 90 applications (Section 5) that shed light on the benefits of the retrofitting program. The first application
 91 estimates the number of lives saved during the Gorkha earthquake as a result of the retrofitting of schools
 92 in Kathmandu Valley since 1997. The second application calculates the annual expected lives saved if the
 93 retrofitting program was extended to all school buildings based on a probabilistic seismic hazard model
 94 we generated for Kathmandu Valley, Nepal. This is followed by Discussion (Section 6) and Conclusion
 95 (Section 7).

2 COUNTERFACTUAL RISK ANALYSIS FRAMEWORK

96 The main idea of counterfactual disaster risk analysis is to explore alternative branches of history to assess
 97 past situations where a disaster might have occurred but was averted or failed to materialise (Woo, 2018).
 98 Impacts associated with a past event, i.e. a realised event, can be expressed as the function of the (a) Hazard,
 99 the likelihood of potentially damaging events, (b) Exposure, the characteristics of assets such as people,
 100 buildings and infrastructure and (c) Vulnerability, the susceptibility of the exposed assets to sustain impact
 101 for a given hazard intensity (UNISDR, 2009). Then, we can write the losses from the realised event as

$$I_{realised} = f(\theta_H, \theta_E, \theta_V), \quad (1)$$

102 where θ_H , θ_E , and θ_V are the hazard, exposure and vulnerability parameters consecutively. Modifications
 103 (δ) of one or multiple parameters that define the realised event allow one to define the impact of a
 104 counterfactual event:

$$I_{counterfactual} = f(\theta_H + \delta_H, \theta_E + \delta_E, \theta_V + \delta_V), \quad (2)$$

105 The purpose of the deviations, δ_H , δ_E , and δ_V , to the realised event's parameters is to explore
 106 counterfactuals. δ_H helps us explore counterfactuals in the hazard (e.g. what if the earthquake had occurred

107 at a slightly different location, or with opposite directivity of rupture?). δ_E helps us explore counterfactuals
 108 in the exposure (e.g. what if the 1906 San Francisco earthquake were to hit today's building stock?). δ_V
 109 helps us explore counterfactuals in vulnerability (e.g. what if all unreinforced masonry buildings had
 110 been retrofitted?). In this paper, we focus on δ_V , while δ_H and $\delta_E = 0$, to highlight the value of effective
 111 vulnerability reduction programs that often go unnoticed.

112 Modelling the impact of events with either Equation 1 or 2 relies on probabilistic risk analysis.
 113 Traditionally used in engineering reliability assessments and performance-based design, probabilistic
 114 risk analysis has been an established approach to assess the risks from natural hazards to entire regions
 115 and cities (Paté-Cornell, 2002; Stergiou and Kiremidjian, 2010). Probabilistic risk analysis systemically
 116 quantifies the potential impacts of hazard events on a system and the likelihood that such consequences
 117 would occur (Bedford et al., 2001). In the case of Equations 1 and 2, the impacts $I_{realised}$ and $I_{counterfactual}$
 118 and their likelihood are obtained through the joint probability of the risk parameters.

119 The expected benefits (B) of effective risk mitigation is then calculated as the difference between the
 120 expected value (the mean) of impacts of the realised event $E(I_{realised})$ and the counterfactual event
 121 $E(I_{counterfactual})$ (see Equation 3 and Figure 1). Assuming the realised impacts are less than those of the
 122 counterfactual, B is expected to be a positive value in Equation 3.

$$B = E(I_{counterfactual}) - E(I_{realised}) \quad (3)$$

3 INVISIBLE SUCCESS OF SEISMICALLY RETROFITTING SCHOOLS IN NEPAL

123 In this paper, we implement the proposed framework to highlight invisible benefits of effective earthquake
 124 risk mitigation. Specifically, we focus on one of the most significant risk interventions in recent years that
 125 led to improved construction practices - the seismic retrofitting of school buildings in Nepal. Amid the
 126 destruction and tragic loss during the Gorkha earthquake, the life-saving benefit of the school retrofitting
 127 was obscured. Likewise if an earthquake event has not yet occurred, retrofitting program may seem like a
 128 waste even though an earthquake may occur at any time. Probabilistic counterfactual risk analysis can be
 129 used to shed light on these invisible benefits.

130 School buildings in Nepal are recognized to be at high risk amidst the region's high seismicity from the
 131 convergence of the Indian tectonic plate with the Eurasian plate, and due to informal construction practices
 132 done with little engineering guidance (Marasini et al., 2020). Damage to school buildings was extensive
 133 from large earthquakes in recent history - the 1988 M_w 6.6 Udayapur earthquake (Gupta, 1988), and the
 134 2011 M_w 6.9 Sikkim/Nepal border earthquake (Rai et al., 2012). The 2015 Gorkha earthquake is a unique
 135 example in terms of the impacts on schools because the earthquake happened on a Saturday, whilst the
 136 school was not in session. Had the earthquake hit on a school day, over one million students would have
 137 been affected (Dixit et al., 2014).

138 Seismic retrofitting of school buildings started in 1997 through the leadership of the National Society for
 139 Earthquake Technology (NSET) as part of Nepal's School Earthquake Safety Program (SESP) (Marasini,
 140 2019). By the time of the Gorkha earthquake in 2015, 300 schools had been retrofitted, 160 of which were
 141 in Kathmandu Valley. It was a big achievement that none of the schools retrofitted under SESP collapsed or
 142 needed major repairs after the earthquake. Because the buildings were found to be structurally sound, all
 143 the retrofitted buildings served as safe shelters and required fewer temporary classrooms (Marasini, 2019).
 144 Following the direction of SESP towards safe learning facilities, the Government of Nepal aims to achieve
 145 minimum school safety criteria nationwide by 2030 through the Comprehensive School Safety Master

146 Plan developed by Nepal's Ministry of Education, Science and Technology (CEHRDC, 2018) based on the
147 global Comprehensive School Safety Framework (UNISDR and GADRRRES, 2017). Recognizing the
148 need to strengthen more than 60,000 school buildings all over Nepal (Marasini et al., 2020), one of the
149 activities in the Master Plan is to retrofit school buildings in earthquake-affected areas.

4 METHODS

4.1 School building database

151 The analyses in this paper are carried out on a database of Nepalese school buildings surveyed and
152 georeferenced in 2013 through the partnership of the Open Data for Resilience Initiative (OpenDRI) and
153 the Government of Nepal with support from Kathmandu Living Labs (OpenDRI, 2012). The building
154 database covers Kathmandu Valley and was produced to understand the seismic risk in the education and
155 health infrastructure. Parts in the dataset related to educational infrastructure were tagged as either *school*,
156 *college*, *university*, or *kindergarten*. The database provides information on the location, number of daytime
157 occupants on a school day, structure type, and whether the school building was retrofitted or not. We chose
158 the OpenDRI dataset for this paper because these building attributes allow us to determine which school
159 buildings were retrofitted under SESP before the 2015 Gorkha earthquake. In addition, the buildings'
160 structure type can be used to identify the buildings' vulnerability, while the number of daytime occupants
161 can be used for fatality calculations.

162 After screening the raw OpenDRI dataset for missing information or non-school buildings, the final
163 dataset we use for this work consists of 5029 school buildings, of which 70 were retrofitted (see Figure 2).
164 We highlight that the OpenDRI dataset we use for this study provides information on only 70 out of the 160
165 retrofitted school buildings identified by NSET in Kathmandu Valley's affected areas (Marasini, 2019). The
166 database consists of buildings with unreinforced masonry-type (URM-type) and reinforced concrete-type
167 (RC-type) structures. The daytime occupancy for the 70 retrofitted schools go up to 800, with a mean of
168 134, whereas the occupancy for the 5029 school buildings go up to 2000 with a mean of 120.

4.2 Building vulnerability modelling

170 A fundamental step in estimating the benefit of a seismic retrofitting intervention involves obtaining
171 the structure's probability to exceed a certain damage level before and after the intervention. This paper
172 focuses only on the collapse damage level since a vast majority of earthquake fatalities worldwide are
173 due to building collapse (Spence, 2007). Collapse fragility curves are used to represent the probability of
174 collapse for a given earthquake intensity and building class.

175 In this work, we have adopted collapse fragility curves developed by other authors to represent the
176 probability of collapse of the buildings in their retrofitted and non-retrofitted states. The collapse fragility
177 curves we use for the Nepalese school building stock in this study are presented in Figure 3. The median η
178 and lognormal standard deviation β of the fragility curves expressed as PGA lognormal distributions are
179 shown in Table 1.

180 For non-retrofitted buildings, we adopt Giordano et al. (2021a)'s empirical-based fragility curves
181 specifically developed for Nepalese school buildings. The curves were generated using a Bayesian
182 approach to incorporate well-established fragility models such as the HAZUS database (Federal Emergency
183 Management Agency, 2015) and World Bank's Structural Integrity and Damage Assessment database
184 (SIDA) that was conducted under the Global Program for Safer Schools (Worldbank, 2019). The collapse
185 fragility curves from Giordano et al. (2021a) were assigned to the buildings in the OpenDRI dataset based
186 on their structure type - unreinforced load-bearing wall schools were assigned the URM collapse fragility
187 curve, while reinforced concrete schools were assigned the RC collapse fragility.

188 For retrofitted buildings, we use the collapse fragility curve developed by Giordano et al. (2021b) for
 189 retrofitted stone masonry buildings in Nepal that are considered to have good quality material. The fragility
 190 curves in Giordano et al. (2021b) were produced analytically using a non-linear static pushover analysis for
 191 stone masonry buildings retrofitted with the 'RC strong-back approach'. It should be noted that the selected
 192 fragility curve for retrofitted school buildings does not necessarily represent the variation in the retrofit
 193 solutions available in Nepal, as well as the workmanship and original quality of the buildings, rather this is
 194 the best information available to the authors at the time of writing.

195 4.3 Expected fatalities from building collapse

196 A vast majority of earthquake fatalities worldwide are due to building collapse (Spence, 2007). Therefore,
 197 this paper focuses on quantifying the fatalities from earthquake-induced building collapse, and the reduced
 198 estimated fatalities from retrofitting interventions.

199 To estimate fatalities due to building collapse, we adopt a semi-empirical casualty model that takes
 200 advantage of the availability of detailed building inventory and collapse fragility curves specific to the
 201 building types in Nepal. The approach is adopted from the semi-empirical forward model implemented in
 202 the USGS Prompt Assessment of Global Earthquakes for Response (PAGER) system (Jaiswal et al., 2011)
 203 for determining the extent of earthquake impacts globally. In contrast to USGS PAGER's use of Modified
 204 Mercalli shaking intensities, the earthquake intensity for this study is expressed in terms of peak ground
 205 accelerations. In this study, we calculate the total estimated fatalities $E[I]$ for a given building portfolio
 206 having a total number of m buildings from a single earthquake event. Each building i in the portfolio has a
 207 known structure type k_i . Using the empirical casualty model, we can write $E[I]$ as

$$208 E[I] = \sum_{i=1}^m O_i \cdot FR_i(k_i) \cdot C_i(im_i, k_i) \quad (4)$$

209 where O_i is the total exposed population inside building i at the time of the earthquake, $FR_i(k_i)$ is the
 210 fatality rate associated with the collapse of building i based on its structure type k_i , and $C_i(im_i, k_i)$ is the
 211 probability of collapse of building i given the earthquake intensity at its location im_i and its structure type
 k_i .

212 A fixed fatality rate of $FR_i(k_i) = 20\%$ for all structure types k_i in the dataset is adopted for the study.
 213 This fatality rate is based on NSET's recommendation for both RC and masonry building classes, of which
 214 all the buildings in the dataset fall into (NSET, 2000). This comes with an assumption that the same level
 215 of casualty is expected regardless of the level of school (e.g. primary or higher grades), nature of escape
 216 routes, or the occupants' level of preparedness.

217 By calculating $E[I]$ for a counterfactual and a realised scenario using Equation 4, and plugging into
 218 Equation 3, we can calculate the expected benefits of effective risk mitigation in terms of lives saved.
 219 In order to generate the entire probability distribution of fatalities, we conduct Bernoulli simulations
 220 (10,000) for collapse given a shaking intensity $C_i(im_i)$ at each building location and for each building
 221 class k_i for both the realised and counterfactual scenario. The complete source code is available at
 222 <https://github.com/ntu-dasl-sg/frontiers2021-PLS>.

5 APPLICATIONS

223 5.1 Lives saved during the 2015 Gorkha earthquake due to the school retrofitting in 224 Kathmandu Valley

225 In order to quantify the reduced fatalities from the school retrofit program in Kathmandu Valley, we
226 estimate the fatalities during the 2015 Gorkha earthquake in the 70 retrofitted school buildings in our
227 database as well as in the counterfactual scenario where these are not retrofitted. By chance, the earthquake
228 occurred during a school holiday, during which occupancy was very low. For both re-analysis scenarios
229 (current retrofit and counterfactual non-retrofit schools), we analyse fatalities for the expected occupancy
230 during the school day. While there were a total of 160 schools retrofitted in Kathmandu Valley at the time
231 of the 2015 Gorkha earthquake (Marasini, 2019), our database contained information on 70. Hence while
232 the focus of our analysis is on the life-saving benefit of the retrofit of the 70 schools in our data, the true
233 reduction in fatalities due to the earthquake retrofitting program is much greater. A map of the 70 retrofitted
234 school buildings used in this analysis is shown in Figure 4.

235 The shaking intensity at the school sites during the 2015 Gorkha earthquake is obtained from the
236 broadband ground-motion simulations produced by Chen and Wei (2019) for the earthquake event. This
237 hazard model was selected because the location of sources of the high-frequency energy (strong-motion
238 generation areas) is a critical factor in explaining the relatively low damage phenomenon observed in
239 Kathmandu Valley during the 2015 Gorkha earthquake (Gallović, 2016; Koketsu et al., 2016), aside from
240 the effects of site conditions and rupture directivity (Dixit et al., 2015; Rajaure et al., 2017; Gallović, 2016;
241 Koketsu et al., 2016). A map of the PGA values at the location of the retrofitted buildings is shown in
242 Figure 4. With this hazard model, PGA values at the location of the retrofitted buildings range from 0.065
243 to 0.149 g, and come in a resolution of 0.0167 degrees, or around 1.85km. More details about the PGA
244 data are summarised in Chen and Wei (2019) and its companion paper, Wei et al. (2018).

245 In order to calculate the estimated impacts in a counterfactual scenario, $E[I]_{counterfactual}$, in which the
246 SESP seismic retrofitting program was absent before the Gorkha earthquake, we use Equation 4 to estimate
247 the total fatalities for the 70 buildings under this counterfactual scenario. The probability of collapse
248 $C_i(im_i, k_i)$ of any building i is obtained from the fragility curve of the building at its *non-retrofitted state*
249 and the Gorkha earthquake event-specific PGA at the building's location im_i . The collapse fragility curves
250 for the non-retrofitted state are assigned as described in Section 4.2, and the PGA values at the building
251 locations are extracted from Chen and Wei (2019)'s hazard model. Using these inputs in Equation 4 results
252 to $E[I]_{counterfactual} = 25$ fatalities.

253 The expected fatalities from the realised event $E[I]_{realised}$ can be calculated using the same approach,
254 but using the collapse fragility curves corresponding to the *retrofitted state* of the buildings as assigned
255 in Section 4.2. This approach results in $E[I]_{realised} = 0$ fatalities, which is the expected total number of
256 fatalities in the realised scenario for the 70 buildings. By comparing the fatalities from the two scenarios as
257 in Equation 3, we estimate that the lives of approximately 25 school occupants were saved in Kathmandu
258 by the retrofit of the 70 schools (see Figure 5).

259 In an attempt to explore the sensitivity of the casualty estimates to different hazard models for the
260 2015 Gorkha earthquake, we repeated the analysis using a PGA map from the USGS ShakeMap (USGS
261 ShakeMap, 2015; Wald and Allen, 2007). While using Chen and Wei (2019)'s hazard model results in 25
262 lives saved, using the USGS ShakeMap hazard model results in 68 lives saved (see Figure S1). The analysis
263 using either model highlights the life-saving benefit of the school retrofitting program, but we believe that
264 the fatality analysis using Chen and Wei (2019)'s model is more accurate in terms of representing the

shaking during the 2015 Gorkha earthquake. Chen and Wei (2019)'s model better captures the amplification or attenuation of the seismic shaking as it accounts for the location of sources of the high-frequency energy (strong-motion generation areas), rupture directivity, and site conditions critical in understanding the relatively low damage phenomenon observed in Kathmandu Valley during the earthquake.

5.2 Annual expected lives saved through scaling the retrofit programs to all schools in Kathmandu Valley

Part of the Comprehensive School Safety Master Plan is the ambition to scale earthquake retrofitting to all vulnerable schools (CEHRDC, 2018). As such, we develop a second case study to better understand the life-saving impact of such a program. We assess expected fatalities if the 5029 schools in Kathmandu Valley were retrofitted, and if they remained in their current state. This analysis is conducted for the entire seismic hazard of Nepal, to better reflect the distribution of potential events to impact Kathmandu Valley.

A probabilistic seismic hazard analysis (PSHA) was developed for the school building sites based on twenty-three independent seismic source zones for Nepal identified by Ram and Wang (2013) and adopted in Chaulagain et al. (2015)'s PSHA model. The ground motion prediction equation by Chiou and Youngs (2014) for active shallow crust regions is used within a logic tree for an event-based probabilistic seismic hazard calculation in the OpenQuake-engine (Silva et al., 2014). To reach statistical convergence, 100,000 stochastic event sets with a 1-year time interval were generated (Silva, 2016). The result of the simulation is a large number of realisations of seismic events and corresponding shaking at the locations of the schools within a year. The resulting hazard curves for some selected schools in the database are shown in Figure 6.

For every event generated, the number of fatalities in the building portfolio due to collapse is estimated using Equation 4. In the fatality calculation of each event, we incorporate the probability distribution of school building occupancy. In Nepal, schools are open and run 220 days a year, and each school day lasts for 6 hours (Government of Nepal, 2009). This means that out of the 8760 hours in a year, 1320 (15%) are school hours in Nepal. To account for this, we simulate a large number of Bernoulli trials for each event that takes a 15% probability of occurring during school hours. The resulting annual fatality exceedance probability curves for two different retrofitting scenarios are shown in Figure 7.

The average annual fatalities are obtained by integrating the hazard curve. For the scenario in which none of the 5029 school buildings is retrofitted, we estimate 13 average annual fatalities, whereas when the retrofitting program is extended to all buildings, we estimate an average of 1 annual fatality. In this probabilistic analysis, we calculate an average of 12 annual lives saved from scaling the retrofit program in all of Kathmandu Valley.

6 DISCUSSION

6.1 A counterfactual analysis approach to celebrate effective risk reduction

In a field focused on long-term resilience to rare (i.e. volatile) hazard events, perceptions of risk are biased by realised outcomes. The perception of *no impacts* when in fact DRM work is successful can result in policymakers and society at large to undervalue the importance of proactive intervention. Shedding light on successes and *what might have been*, not only recognizes the outstanding work of those working to reduce risk, but is also a crucial component of encouraging decision-makers to continue investments in measures that keep our communities safe.

We highlight the need to celebrate the often invisible successes of disaster risk reduction interventions, in order to incentivise, better learn and replicate investments in such interventions. We further propose

305 and demonstrate the use of a probabilistic counterfactual risk analysis framework to identify, quantify
306 and highlight these invisible successes. The framework demonstrates that judgement of a risk reduction
307 intervention should be based on a broad exploration of possible outcomes, not only on specific outcomes.

308 We demonstrated two applications of the probabilistic downward counterfactual risk analysis to (1)
309 celebrate lives saved by a disaster risk reduction intervention (earthquake school retrofitting) amidst a
310 past event (the 2015 Gorkha earthquake in Nepal), and (2) assess expected annual lives saved due to
311 the intervention with the use of a probabilistic hazard model. The two applications show that even in
312 the midst of a tragic disaster, or if a hazard event has not occurred yet, there are often successes in risk
313 reduction intervention to celebrate. The counterfactual analysis showed that numerous expected fatalities
314 were avoided during the Gorkha earthquake because of the government-led retrofitting of school buildings
315 starting in 1997, and many more could be saved if the retrofit program were scaled to all schools in
316 Kathmandu Valley.

317 **6.2 Lives saved as a risk reduction benefit metric**

318 In our demonstrations, the risk benefit of DRM intervention is measured in terms of a reduction in
319 loss of life - the first target metric within the Sendai Framework For Disaster Risk Reduction (UNISDR,
320 2015). A risk benefit metric in financial units can also be used, as with a typical cost-benefit analysis.
321 However such analysis tends to highlight interventions that effectively protect high-value areas instead of
322 high-vulnerability areas, which exacerbates inequities (Markhvida et al., 2020; Lallement et al., 2020).

323 More alternative risk reduction benefit metrics for this analysis include the number of displaced people,
324 business downtime, damage to buildings and cultural heritage, psychological distress and more. For
325 the Nepal case study, for example, the benefits of retrofitting go well beyond the reduced physical
326 vulnerability of the buildings. Retrofitted schools served as immediate community shelters, field hospitals
327 and relief centres. Classes in the retrofitted buildings were operated without fear, resulting in less demand
328 for temporary classrooms (Marasini et al., 2020). Loss avoidance is not the only invisible benefit of
329 disaster mitigation, and the benefits of DRM interventions go beyond reduction of impact. Certain
330 intervention designs can have co-benefits such as retrofit programs that improve the environmental comfort
331 of classrooms, that serve as training platforms to local constructors who replicate the methods in other
332 building constructions, or that are linked with student and teacher earthquake preparedness programs
333 (Spence and So, 2021).

334 **6.3 First order approach**

335 The analyses and estimates of lives saved presented are first order and serve as proof of concept of the
336 counterfactual framework to highlight successes in DRM. Following are limitations that need to be noted
337 for future work:

- 338 • The analysis did not account for fatalities from partially collapsed buildings. To account for this, one
339 may use NSET's recommendation to use a 10% fatality rate for heavily damaged buildings (NSET,
340 2000)
- 341 • The building portfolio dataset we use in the two case studies is only a subset of all the schools within
342 the study area. The dataset used for the first case study (Section 5.1) contains only 70 out of the 160
343 retrofitted schools in Kathmandu Valley. For the second case study (Section 5.2), we also did not
344 include school building data that has no information on the occupancy and structure type.

- 345 • For the second case study, the assumption that all 5,029 school buildings will be retrofitted seems in
346 line with the plans of the Government of Nepal. However, it is not a forecast of the future, as much
347 uncertainty remains. We hope that our analysis serves to support policy decisions for more resilient
348 schools.

349 **6.4 Broader applications with other domains of hazard and interventions**

350 Probabilistic downward counterfactual risk analysis has potential for application to other hazards. A
351 key step of the framework is to identify which risk component the intervention influences. Earthquake
352 risk reduction, for example, influences either the reduction of exposure or vulnerability. Measures such as
353 restricting development in high-hazard zones decrease exposure, whereas better construction standards
354 decrease the structural vulnerability of buildings and infrastructure.

355 Beyond earthquake risk reduction, the proposed framework can also be used in other domains of hazard.
356 Following are a few selected examples of natural hazards and corresponding interventions that could
357 be celebrated using counterfactual analysis. Enclosed in parenthesis are the risk component/s that the
358 intervention influences.

359 **1. Earthquake**

- 360 • Reconstruction and seismic retrofit (Vulnerability)
- 361 • Construction inspection (Vulnerability)
- 362 • Preparedness exercises (Exposure, Vulnerability)

363 **2. Tropical cyclone and Tsunami**

- 364 • Early warning system and timely announcements (Exposure)
- 365 • Evacuation and provision of temporary shelters (Exposure and Vulnerability)
- 366 • Public awareness about the hazard (Exposure and Vulnerability)

367 **3. Flood**

- 368 • Limiting urban development in flood-prone zones (Exposure, Vulnerability)
- 369 • Enhanced flood management infrastructure (Exposure, Hazard)
- 370 • Timely emergency response (Vulnerability, Exposure)
- 371 • Preservation or restoration of natural ecosystems for flood mitigation (Hazard)

372 **4. Landslides**

- 373 • Early warning system via geodynamic monitoring (Exposure)
- 374 • Mitigation infrastructure, e.g. drainage systems (Exposure, Hazard)

375 **5. Wildfires**

- 376 • Early warning system via dynamic weather forecasts (Exposure)

7 CONCLUSION

377 This study combines the probabilistic risk analysis framework and counterfactual analysis to quantify and
378 highlight the significant benefits of successful disaster risk reduction interventions that often go unnoticed.
379 By using an appropriate counterfactual scenario as a baseline against which to compare realised outcomes,
380 it makes clear that the impact of hazards would be much worse without important investments in risk
381 reduction.

382 Using this approach, we demonstrate that an estimated 25 lives were saved (probabilistically) during
383 the 2015 Gorkha earthquake from the retrofitting of 70 schools in Kathmandu Valley alone. If such a

384 retrofitting program were scaled to all the approximately 5,029 schools in Kathmandu Valley, we estimate
385 a reduction of 12 annual school children fatalities based on the significant seismic hazard of the region.
386 These are clearly important programs that should be prioritized, celebrated, scaled, and replicated in areas
387 with high seismic risk.

388 Loss of life reduction is an important metric for risk reduction, not only because the life-safety of children
389 and all people is paramount, but also because doing so centres attention on high-vulnerability areas and
390 buildings, even if the financial losses associated may be small. However loss-avoidance is not the only
391 invisible benefit of disaster mitigation, and the many co-benefits can also be included to further highlight
392 the value of risk reduction interventions.

393 While this study demonstrates the application of probabilistic counterfactual risk analysis to quantify
394 the life-saving value of a school earthquake retrofitting program in Kathmandu Valley, the methodology
395 can be used in other contexts and hazards. Programs for typhoon and tsunami early warning, hazard
396 informed urban development planning, flood-management through nature-based solution are all examples
397 of important programs whose true benefits could be more accurately valued through the use of probabilistic
398 counterfactual analysis. In so doing, such analysis would provide increased incentives to invest in risk
399 reduction programs, learn from ones with demonstrated success, and serve to encourage those whose
400 humble work is critically important even when often unnoticed.

CONFLICT OF INTEREST STATEMENT

401 The authors declare that the research was conducted in the absence of any commercial or financial
402 relationships that could be construed as a potential conflict of interest.

AUTHOR CONTRIBUTIONS

403 MR lead the writing, research and analysis of both case studies. All authors contributed to the
404 conceptualisation and design of the study. DL conceived of the idea of celebrating successes in disaster risk
405 reduction using counterfactual analysis. YL and DL provided critical feedback that shaped the research,
406 analysis and manuscript.

FUNDING

407 This project is supported by the National Research Foundation, Prime Minister's Office, Singapore under
408 the NRF-NRFF2018-06 award, the Earth Observatory of Singapore, the National Research Foundation of
409 Singapore, and the Singapore Ministry of Education under the Research Centers of Excellence initiative.
410 MR is supported by a PhD scholarship from the Earth Observatory of Singapore.

ACKNOWLEDGMENTS

411 We thank Dr. Nama Budhathoki, Kathmandu Living Labs and the GFDRR Open Data for Resilience
412 Initiative for data on school buildings in Nepal. We also thank Dr. Shengji Wei and Dr. Meng Chen for
413 data and information on the broadband simulations in Kathmandu for the 2015 Gorkha earthquake, and Dr.
414 Michele Nguyen for the guidance on the use of the OpenQuake engine.

SUPPLEMENTAL DATA

DATA AVAILABILITY STATEMENT

415 The original contributions presented in the study are included in the article. The complete source code
 416 for the analysis is available at <https://github.com/ntu-dasl-sg/frontiers2021-PLS>. Further inquiries can be
 417 directed to the corresponding author/s.

REFERENCES

- 418 Aspinall, W. and Woo, G. (2019). Counterfactual analysis of runaway volcanic explosions. *Frontiers in*
 419 *Earth Science* 7, 222
- 420 Bedford, T., Cooke, R., et al. (2001). *Probabilistic risk analysis: foundations and methods* (Cambridge
 421 University Press)
- 422 CEHRDC (2018). Comprehensive School Safety Minimum Package: Volume 1 – Report. Sano Thimi,
 423 Bhaktapur, Nepal: Centre For Education and Human Resource Development Accessed 2021-12-20.
 424 <https://www.preventionweb.net/publication/nepal-comprehensive-school-safety-minimum-package>
- 425 Chaulagain, H., Rodrigues, H., Silva, V., Spacone, E., and Varum, H. (2015). Seismic risk assessment and
 426 hazard mapping in nepal. *Natural Hazards* 78, 583–602
- 427 Chen, M. and Wei, S. (2019). The 2015 Gorkha, Nepal, earthquake sequence: II. broadband simulation of
 428 ground motion in Kathmandu. *Bulletin of the Seismological Society of America* 109, 672–687
- 429 Chiou, B. S.-J. and Youngs, R. R. (2014). Update of the chiou and youngs nga model for the average
 430 horizontal component of peak ground motion and response spectra. *Earthquake Spectra* 30, 1117–1153
- 431 Dixit, A. M., Ringler, A. T., Sumy, D. F., Cochran, E. S., Hough, S. E., Martin, S. S., et al. (2015).
 432 Strong-motion observations of the M 7.8 Gorkha, Nepal, earthquake sequence and development of the
 433 N-SHAKE strong-motion network. *Seismological Research Letters* 86, 1533–1539
- 434 Dixit, A. M., Yatabe, R., Dahal, R. K., and Bhandary, N. P. (2014). Public school earthquake safety
 435 program in Nepal. *Geomatics, Natural Hazards and Risk* 5, 293–319
- 436 Federal Emergency Management Agency (2015). 2.1 earthquake model technical manual. *Federal*
 437 *Emergency Management Agency, Washington, DC*
- 438 Gallovič, F. (2016). Modeling velocity recordings of the M w 6.0 South Napa, California, earthquake:
 439 Unilateral event with weak high-frequency directivity. *Seismological Research Letters* 87, 2–14
- 440 Giordano, N., De Luca, F., Sextos, A., Ramirez Cortes, F., Fonseca Ferreira, C., and Wu, J. (2021a).
 441 Empirical seismic fragility models for nepalese school buildings. *Natural Hazards* 105, 339–362
- 442 Giordano, N., Norris, A., Manandhar, V., Shrestha, L., Paudel, D. R., Quinn, N., et al. (2021b). Financial
 443 assessment of incremental seismic retrofitting of nepali stone-masonry buildings. *International Journal*
 444 *of Disaster Risk Reduction* 60, 102297
- 445 Government of Nepal (2009). School sector reform plan 2009-2015 Accessed 2022-03-28.
 446 https://www.moe.gov.np/assets/uploads/files/SSRP_English.pdf
- 447 Gupta, S. P. (1988). *Report on eastern Nepal earthquake 21 August 1988: Damages and recommendations*
 448 *for repairs and reconstruction* (Asian Disaster Preparedness Center, Asian Institute of Technology)
- 449 Jaiswal, K., Wald, D. J., Earle, P. S., Porter, K. A., and Hearne, M. (2011). Earthquake casualty models
 450 within the usgs prompt assessment of global earthquakes for response (pager) system. In *Human*
 451 *casualties in earthquakes* (Springer). 83–94
- 452 Koketsu, K., Miyake, H., Guo, Y., Kobayashi, H., Masuda, T., Davuluri, S., et al. (2016). Widespread
 453 ground motion distribution caused by rupture directivity during the 2015 Gorkha, Nepal earthquake.
 454 *Scientific reports* 6, 1–9
- 455 Lallemand, D., Loos, S., McCaughey, J. W., Budhathoki, N., and Khan, F. (2020). *Informatics for*
 456 *Equitable Recovery: Supporting equitable disaster recovery through mapping and integration of social*

- 457 vulnerability into post-disaster impact assessments. Tech. rep. doi:10.32656/IER_Final_Report_2020
- 458 Lallemand and Rabonza, Lin, Y., Tadepalli, S., Wagenaar, D., Michele, N., Choong, J., et al. (2022).
459 Sheding light on avoided disasters: Measuring the invisible benefits of disaster risk management using
460 probabilistic counterfactual analysis. *Global Assessment Report on Disaster Risk Reduction 2022*
461 <https://hdl.handle.net/10356/153502>
- 462 Lin, Y. C., Jenkins, S. F., Chow, J. R., Biass, S., Woo, G., and Lallemand, D. (2020). Modeling downward
463 counterfactual events: Unrealized disasters and why they matter. *Frontiers in Earth Science*, 443
- 464 Marasini, N. (2019). NSET Experiences on Safer Schools Initiative. In *Asian Conference on Disaster
Reduction, Ankara, Republic of Turkey* (ACM). Accessed 20 Nov 2021. <https://bit.ly/32P4pjC>
- 465 Marasini, N., Shrestha, S., Guragain, R., Shrestha, H., Prajapati, R., and Khatiwada, P. (2020). Enhancing
466 earthquake safety of schools: Lessons learned from Nepal. In *Proceedings of the 17th World Conference
on Earthquake Engineering* (Sendai, Japan), Article No. 3g–0023
- 467 Markhvida, M., Walsh, B., Hallegatte, S., and Baker, J. (2020). Quantification of disaster impacts through
468 household well-being losses. *Nature Sustainability* 3, 538–547. doi:10.1038/s41893-020-0508-7.
469 Number: 7 Publisher: Nature Publishing Group
- 470 Mileti, D. (1999). *Disasters by design: A reassessment of natural hazards in the United States* (Joseph
471 Henry Press)
- 472 Moore, H. E. (1958). Tornadoes over Texas: A study of Waco and San Angelo in disaster.
- 473 NSET (2000). *Seismic vulnerability of the public-school buildings of Kathmandu Valley and methods for
reducing it*. Tech. rep. <https://nset.org.np/nset2012/images/publicationfile/20130724114208.pdf>
- 474 OpenDRI (2012). *Understanding Nepal's Risks" Open Data for Resilience Initiative Project*. Tech. rep.,
475 Open Data for Resilience Initiative Project. <https://opendri.org/project/nepal/>
- 476 Oughton, E. J., Ralph, D., Pant, R., Leverett, E., Copic, J., Thacker, S., et al. (2019). Stochastic
477 counterfactual risk analysis for the vulnerability assessment of cyber-physical attacks on electricity
478 distribution infrastructure networks. *Risk Analysis* 39, 2012–2031
- 479 Paté-Cornell, E. (2002). Risk and uncertainty analysis in government safety decisions. *Risk analysis* 22,
480 633–646
- 481 Rai, D. C., Mondal, G., Singhal, V., Parool, N., Pradhan, T., and Mitra, K. (2012). Reconnaissance report
482 of the m6. 9 sikkim (india–nepal border) earthquake of 18 september 2011. *Geomatics, Natural Hazards
and Risk* 3, 99–111
- 483 Rajaure, S., Asimaki, D., Thompson, E. M., Hough, S., Martin, S., Ampuero, J., et al. (2017).
484 Characterizing the Kathmandu Valley sediment response through strong motion recordings of the
485 2015 Gorkha earthquake sequence. *Tectonophysics* 714, 146–157
- 486 Ram, T. D. and Wang, G. (2013). Probabilistic seismic hazard analysis in nepal. *Earthquake Engineering
and Engineering Vibration* 12, 577–586
- 487 Robson, D. (2019). The bias that can cause catastrophe. *BBC*
- 488 Roese, N. J. (1997). Counterfactual thinking. *Psychological bulletin* 121, 133
- 489 Shepherd, T. G., Boyd, E., Calel, R. A., Chapman, S. C., Dessai, S., Dima-West, I. M., et al. (2018).
490 Storylines: an alternative approach to representing uncertainty in physical aspects of climate change.
491 *Climatic change* 151, 555–571
- 492 Silva, V. (2016). Critical issues in earthquake scenario loss modeling. *Journal of Earthquake Engineering*
493 20, 1322–1341
- 494 Silva, V., Crowley, H., Pagani, M., Monelli, D., and Pinho, R. (2014). Development of the OpenQuake
495 engine, the Global Earthquake Model's open-source software for seismic risk assessment. *Natural
496 Hazards* 72, 1409–1427

Table 1. Fragility curve parameters adopted in the analysis for the school buildings in the OpenDRI database. The parameters follow a lognormal model where η (g) is the median PGA and β is the lognormal standard deviation.

Reference	Building class	Structural state of building	Collapse state parameters	
			η	β
(Giordano et al., 2021a)	Non-retrofitted URM - Unreinforced masonry bearing wall, low-rise (pre-code)	Un-retrofitted	0.55	0.76
(Giordano et al., 2021a)	Non-retrofitted RC - Concrete frame buildings with unreinforced masonry infill walls, low-rise (low code)	Un-retrofitted	1.13	0.84
(Giordano et al., 2021b)	Retrofitted stone masonry buildings	Retrofitted	1.133	0.452

- 502 Smith, D. (2005). *Through a glass darkly-a response to Stallings’’ Disaster, Crisis, Collective Stress, and*
 503 *Mass Deprivation*”, vol. 2 (Xlibris Press)
- 504 Spence, R. (2007). Saving lives in earthquakes: successes and failures in seismic protection since 1960.
 505 *Bulletin of Earthquake Engineering* 5, 139–251
- 506 Spence, R. and So, E. (2021). *Why Do Buildings Collapse in Earthquakes?: Building for Safety in Seismic*
 507 *Areas* (John Wiley & Sons)
- 508 Stergiou, E. C. and Kiremidjian, A. S. (2010). Risk assessment of transportation systems with network
 509 functionality losses. *Structure and Infrastructure Engineering* 6, 111–125
- 510 UNISDR (2009). *United Nations Office for Disaster Risk Reduction, UNISDR Terminology and Disaster*
 511 *Risk Reduction*. Tech. rep., United Nations International Strategy for Disaster Reduction, Geneva,
 512 Switzerland
- 513 UNISDR (2015). Sendai framework for disaster risk reduction 2015-2030. In *Third United Nations World*
 514 *Conference on Disaster Risk Reduction (WCDRR)—Resilient People. Resilient Planet*.
- 515 UNISDR and GADRRRES (2017). Comprehensive school safety. united nations international strategy
 516 for disaster reduction and global alliance for disaster risk reduction resilience in the education sector
 517 Accessed 2021-12-20. <http://gadrrres.net/uploads/files/resources/CSS-Framework-2017.pdf>
- 518 USGS ShakeMap (2015). M 7.8 - 67 km nne of bharatpur, nepal. *USGS ShakeMap Earthquake Hazards*
 519 *Program* [Https://earthquake.usgs.gov/earthquakes/eventpage/us20002926/shakemap/pga](https://earthquake.usgs.gov/earthquakes/eventpage/us20002926/shakemap/pga)
- 520 Wald, D. J. and Allen, T. I. (2007). Topographic slope as a proxy for seismic site conditions and
 521 amplification. *Bulletin of the Seismological Society of America* 97, 1379–1395
- 522 Wei, S., Chen, M., Wang, X., Graves, R., Lindsey, E., Wang, T., et al. (2018). The 2015 Gorkha (Nepal)
 523 earthquake sequence: I. Source modeling and deterministic 3D ground shaking. *Tectonophysics* 722,
 524 447–461
- 525 Woo, G. (2018). Counterfactual disaster risk analysis. *Variance* 10, 279–291
- 526 Woo, G. (2019). Downward counterfactual search for extreme events. *Frontiers in Earth Science* 7, 340
- 527 Woo, G., Maynard, T., and Seria, J. (2017). Reimagining history: counterfactual risk analysis. *Lloyd’s*
 528 *emerging risk report, London*
- 529 Woo, G. and Mignan, A. (2018). Counterfactual analysis of runaway earthquakes. *Seismological Research*
 530 *Letters* 89, 2266–2273
- 531 Worldbank (2019). Global library of school infrastructure. *Global Program for Safer Schools*
 532 <Https://gpss.worldbank.org/en/glosi/about-glosi>

FIGURE CAPTIONS

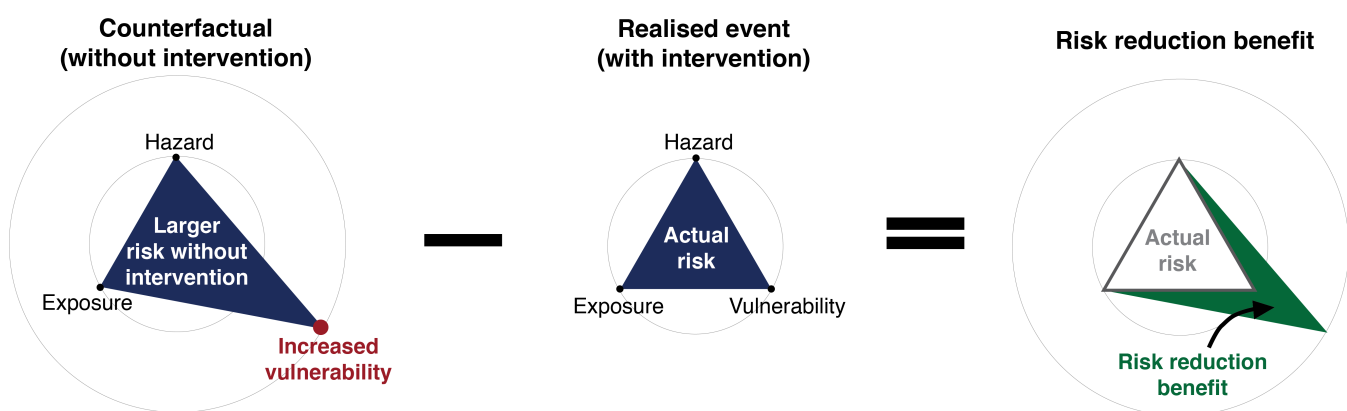


Figure 1. The concept of the counterfactual risk analysis framework for quantifying the probabilistic benefits of effective risk reduction. This graphic serves as a demonstration of the framework that is specific for a risk intervention that reduces vulnerability.

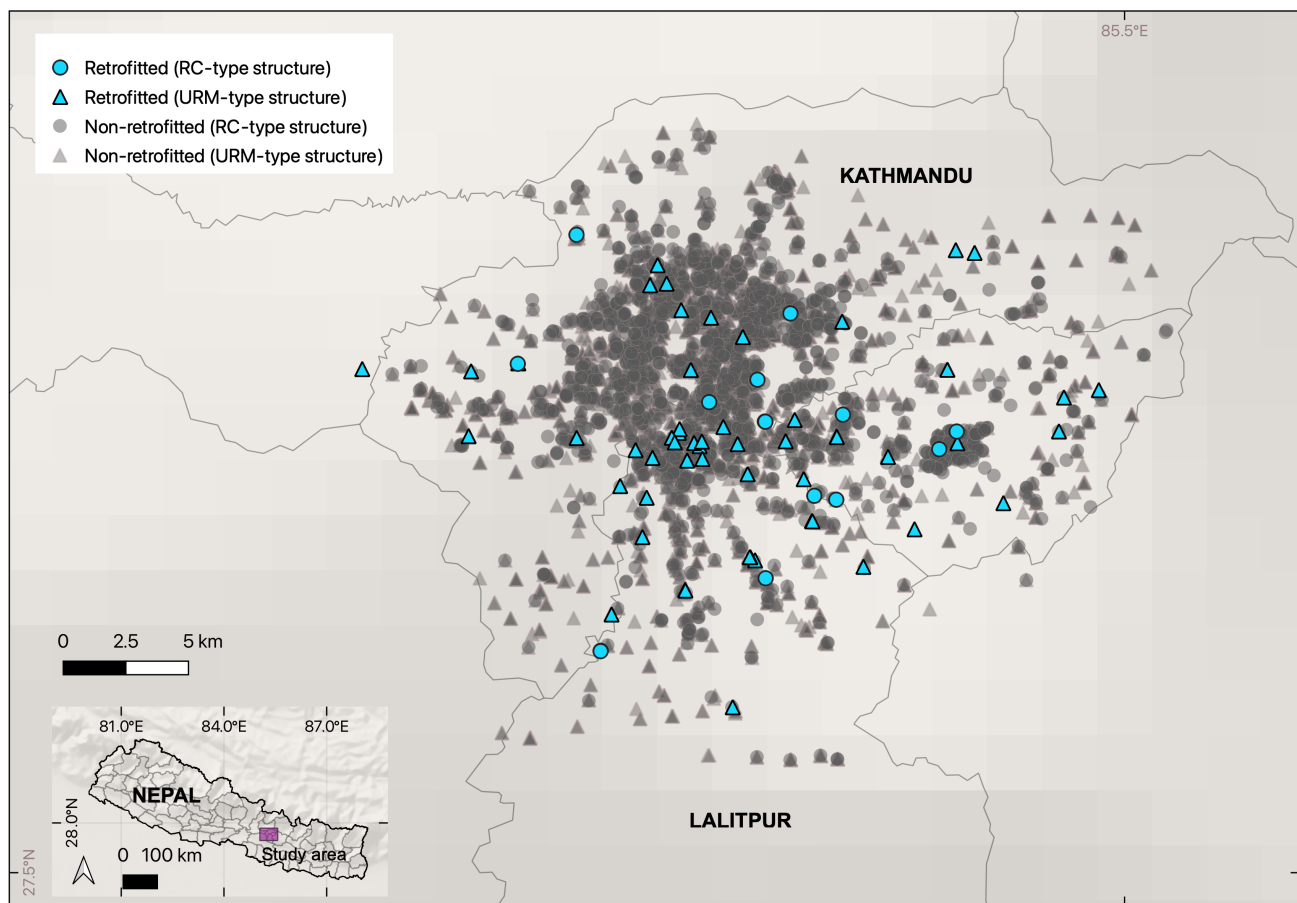


Figure 2. A map of the building database used in the analysis showing distribution of schools retrofitted and non-retrofitted as well as structure type.

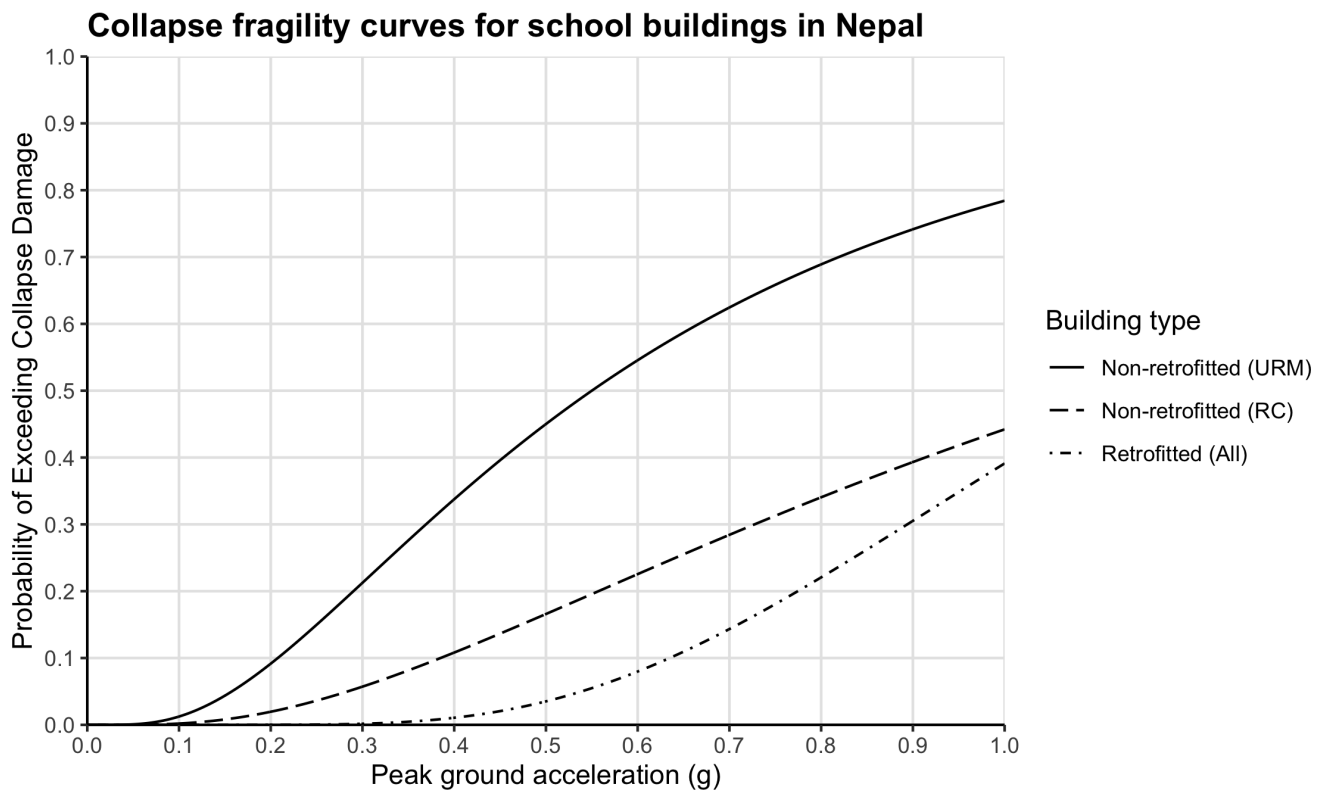


Figure 3. Collapse fragility curves adopted in the analysis.

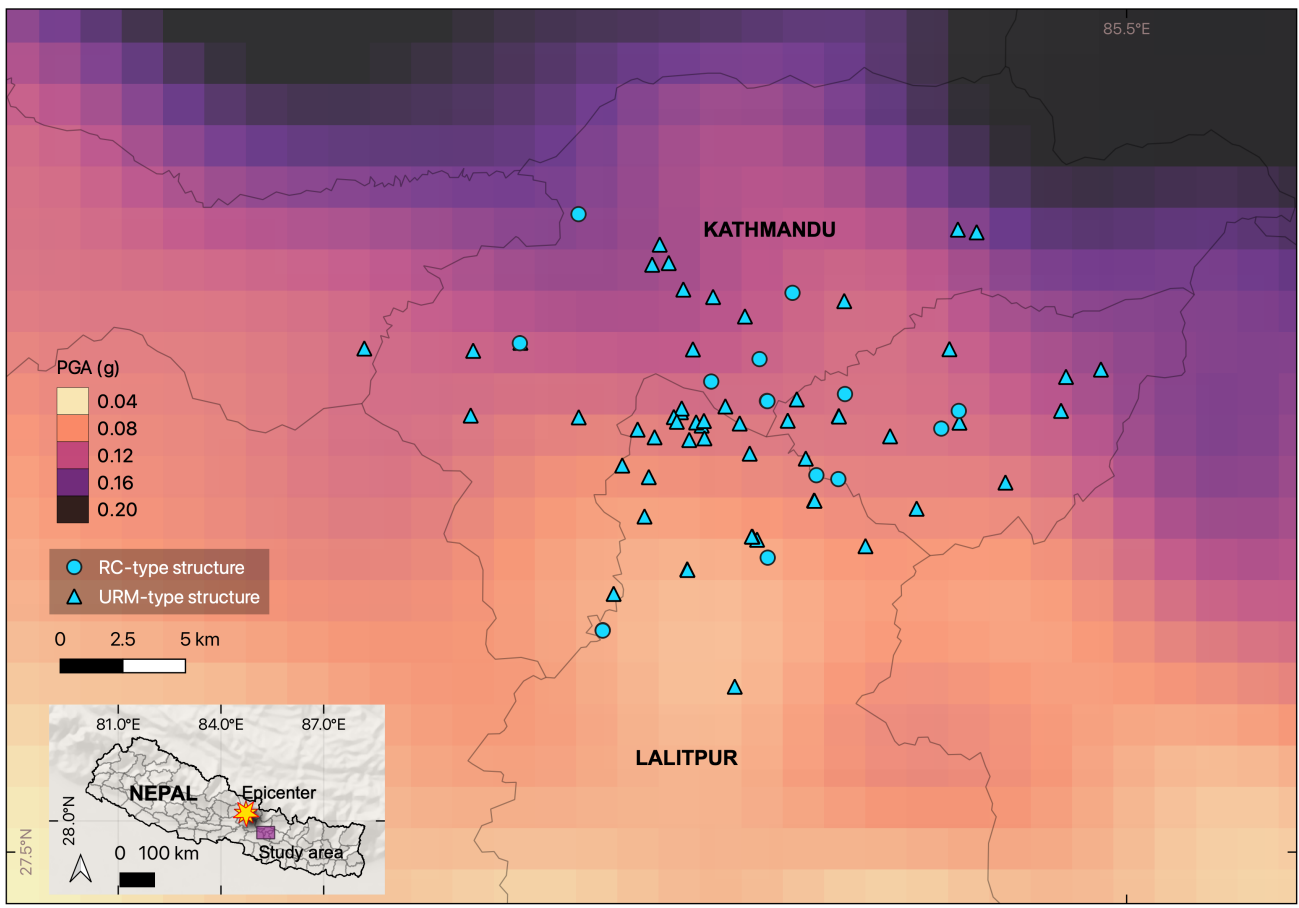


Figure 4. A map of the 70 retrofitted schools and their corresponding structure type used in the analysis described in Section 5.1. The basemap shows the hazard model developed by Chen and Wei (2019) for the 2015 Gorkha earthquake in terms of peak ground acceleration (in g-units).

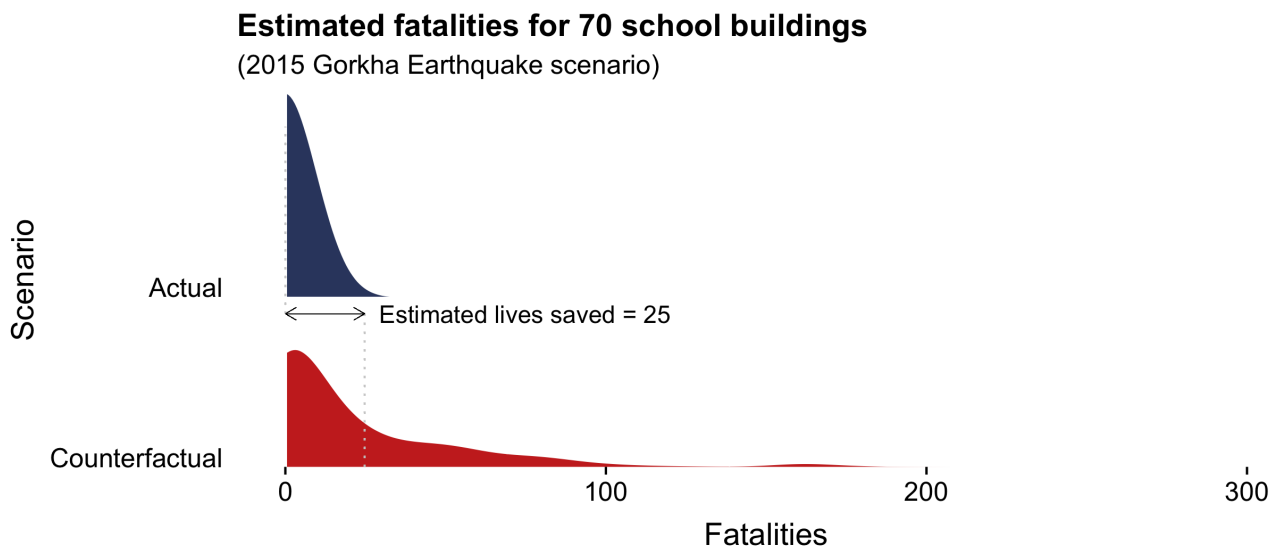


Figure 5. Distribution of estimated fatalities from the 2015 M_w 7.8 Gorkha earthquake based on earthquake intensity values from Chen and Wei (2019). Two scenarios are shown: the actual scenario where all 70 school buildings were retrofitted prior to the 2015 Gorkha earthquake, and a counterfactual scenario where the schools were not retrofitted. Our analysis show an estimated 25 lives in the 70 retrofitted schools.

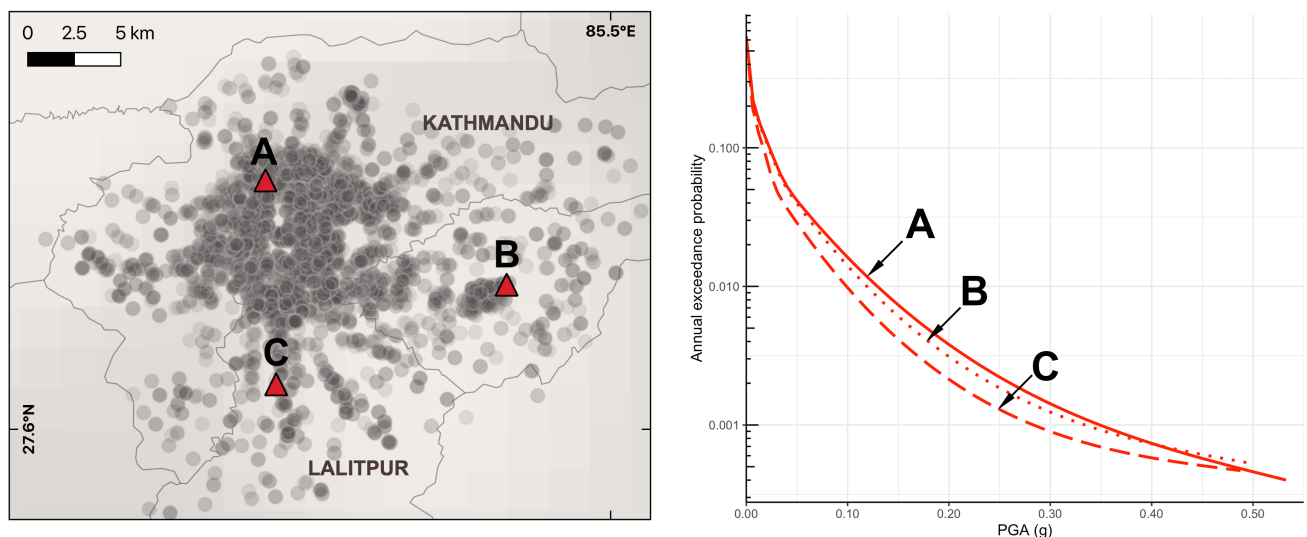


Figure 6. Hazard curves for three sample school building locations in the analysis.

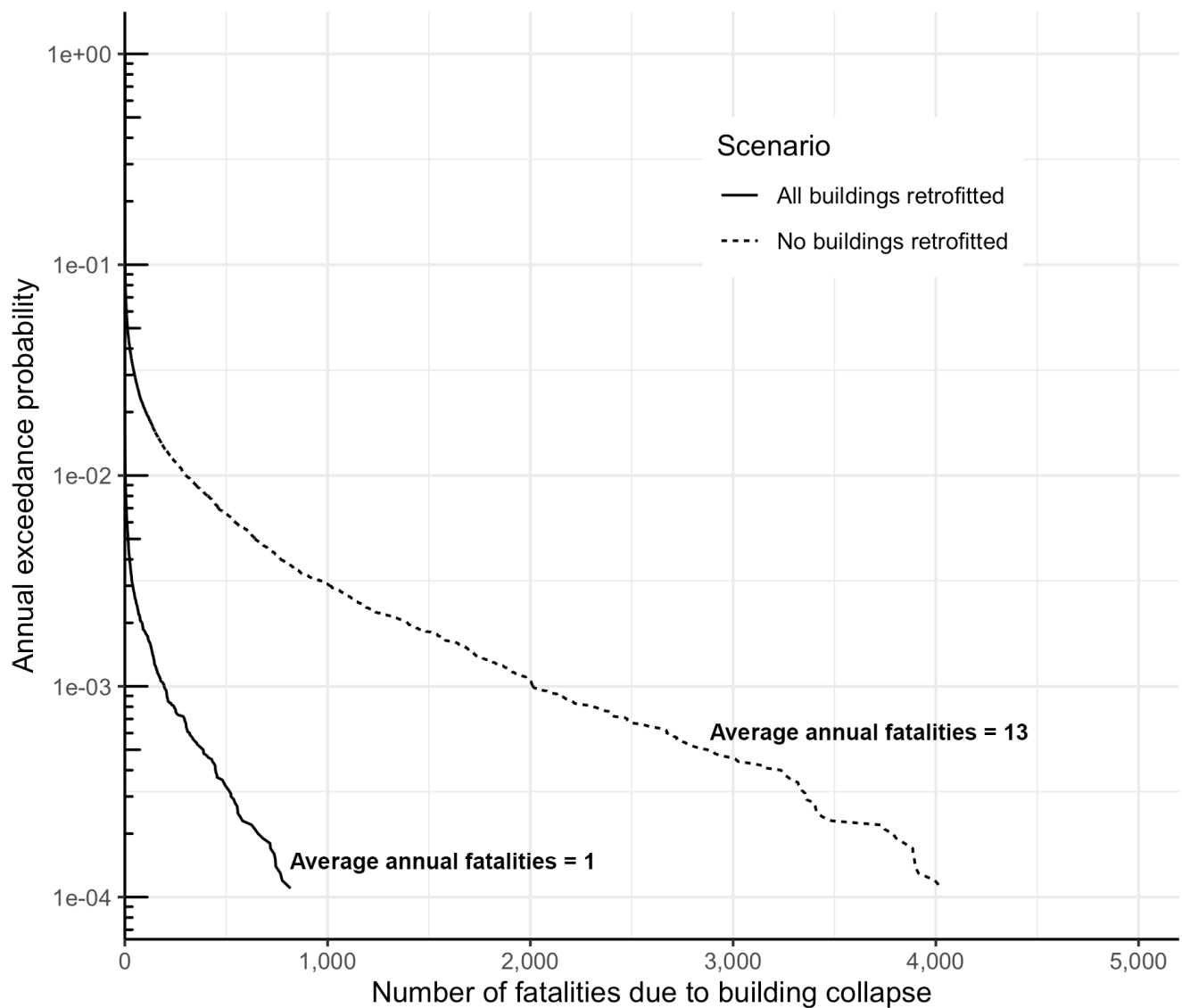


Figure 7. Benefits of extending Nepal's school retrofit program to 5029 schools in the database in terms of the shift in the annual fatality exceedance curve.